# Evidence for High-Efficiency Laser-Heated Hohlraum Performance at 527 nm

R. M. Stevenson,[1] K. Oades,[1] B. R. Thomas,[1] M. Schneider,[2] G. E. Slark,[1] L. J. Suter,[2] R. Kauffman,[2] D. Hinkel,[2] and M. C. Miller[3]

[1]*Atomic Weapons Establishment, Aldermaston, Reading, Berkshire RG7 4PR, United Kingdom*
[2]*Lawrence Livermore National Laboratory, P.O. Box 808, Livermore, California 94551, USA*
[3]*Los Alamos National Laboratory, P.O. Box 1633, Los Alamos, New Mexico 87545, USA*

(Received 8 August 2004; published 10 February 2005)

A series of experiments conducted on the HELEN laser system [M. J. Norman *et al.*, Appl. Opt. **41**, 3497 (2002)], into thermal x-ray generation from hohlraum targets using 527 nm ($2\omega$) wavelength laser light, has shown that it is possible to exceed radiation temperatures previously thought limited by high levels of superthermal or hot electron production or stimulated backscatter. This Letter questions whether the assumptions traditionally applied to hohlraum design with respect to hot plasma filling and the use of $2\omega$ light are too conservative.

DOI: 10.1103/PhysRevLett.94.055006 PACS numbers: 52.38.–r

*Introduction.*—A major factor limiting the radiation temperature achieved within laser-heated hohlraums used in high energy-density physics experiments [1–3] is the onset of parametric instability growth. Traditionally, target design has been guided by the belief that instability growth and the associated deleterious production of energetic electrons can be minimized by ensuring that plasma filling of the hohlraum void to an electron density greater than $1/10$ critical does not occur until the end of the laser pulse. Historical evidence pointed to the interrelationship between the Raman instability and the formation of ''hot'' electrons [4]. Therefore, minimizing the potential for the growth of stimulated Raman scatter (SRS) (electron plasma waves) and stimulated Brillouin scatter (SBS) (ion acoustic waves) instabilities [5,6] became the norm for target design. Under these conditions, the scaling of laser hohlraum performance is well understood [7,8]. This tenet has also guided laser facility operation into the near-UV, as the instability thresholds scale with both focused intensity and wavelength [5]. The experiments reported here investigate the validity of the traditional assumptions as a function of hohlraum size and beam smoothing with $2\omega$ light.

Our motivation for this work is the potential to perform a wide range of high energy-density experiments at $2\omega$. In stating this we note three key points. First, operation of National Ignition Facility [9] at 527 nm would permit access to a far wider operating envelope, potentially allowing high gain fusion [10]. Second, the use of $2\omega$ light for interaction experiments has not been as extensively studied as $1\omega$ and $3\omega$, and anticipated performance is based on limited past data [11–16]. Finally, systematic data on energetic electron production and its relevance to hohlraum performance are required to guide future experimental and facility design.

The experiments discussed here are divided into two series. The first obtained data on the generation of energetic (hot) electrons in hohlraums expected to have higher than usual coronal plasma filling. The second measured the thermal x-ray temperature and stimulated backscatter production as a function of hohlraum size. These two sets of experiments provide a systematic study of hohlraum performance at 527 nm, allowing a detailed comparison with expectations and modeling.

*Experiment.*—The HELEN laser system comprises two opposing beams of wavelength 527 nm with variable pulse shaping capability and energy of up to 400 J per beam [17]. For the first experimental series, both beams were used to heat opposite sides of two sizes of ''empty,'' cylindrical gold hohlraums. The hohlraums were, respectively, 450 $\mu$m long, 450 $\mu$m in diameter and 600 $\mu$m long, 600 $\mu$m in diameter with a wall thickness of 25 $\mu$m. The laser beams were incident at an angle of 45° and the targets had laser entry holes (LEH) that were 100% of their diameter. These were fired with Gaussian pulses of duration of 100 ps, 600 ps, and 1 ns (FWHM).

The goal of the first series was to fill the target with plasma [whose electron density was greater than 10% the critical value ($n_c$) for $2\omega$ light] early in the laser pulse with the express aim of converting significant fractions of the laser energy into hot electrons (i.e., high $f_{\mathrm{hot}}$).

An estimate of $f_{\mathrm{hot}}$ for given hohlraum targets can be made from the degree of plasma filling from the general formula reproduced below [7]. This equation assumes that the energy delivered, after the hohlraum is filled to about $0.1n_c$, appears as hot electrons:

$$f_{\mathrm{hot}} = \frac{1}{2}\exp\left[\frac{-A^2(\mathrm{mm}^4)}{C\lambda^2(\mu\mathrm{m}^2)E(\mathrm{kJ})t_p(\mathrm{ns})}\right]. \quad (1)$$

The variable $C$ takes into account modifying a 1D planar expansion of the plasma from the wall to allow for convergence within cylindrical targets and typically has values within the range ~15–30 depending on the length to diameter ratio of the target. $A$ is the wall area of the target.

 

In the second series of experiments, the targets were axis-symmetric, empty, gold ''halfraums'' whose sizes were scaled to that of a NOVA scale 1 halfraum (1600 $\mu$m diameter $\times$ 1350 $\mu$m long with 25 $\mu$m wall thickness) and were fired with a single axial beam with a 1 ns ''flat top'' pulse shape. The focusing system had a nominal focal ratio of 3.2, and targets were fired under various focal conditions including the use of phased zone plates (PZP) [18] to investigate beam smoothing with particular attention to scale 0.15 and 0.2 halfraums. The PZP designed to produce a 125 $\mu$m diameter focal spot gave a 180 $\mu$m diameter spot thus precluding its use with the scale 0.1 targets (160 $\mu$m LEH).

Three principal diagnostic measurements were made. The backscatter was determined using a full aperture backscatter system (FABS) [19,20] comprising time-integrated energy and time-resolved spectral measurements, and a near backscatter imaging system (NBI) [21]. $f_{\mathrm{hot}}$ was calculated from the hard x-ray bremsstrahlung spectrum resulting from the interaction of these electrons with the target walls. This spectrum was measured with a calibrated ''filter fluorescer'' [22]. Time-resolved measurements of the radiation temperature were made with vacuum x-ray diodes (XRD) [23], filtered to provide an approximately flat response between 0.2 and 1.5 keV, and a diamond photoconductive detector [24]. The XRD photocathodes are routinely calibrated [25] with an estimated error in radiation temperature of $\pm 10\%$.

*Results.*—Table I summarizes the results obtained from the first series of experiments. The calculated values of $f_{\mathrm{hot}}$ have been determined after subtraction of the measured backscatter energy. The measured values for $f_{\mathrm{hot}}$ are significantly at odds with those determined from Eq. (1). Historically it was thought that an enhancement of SRS through poor beam quality and high local irradiance might contribute to high $f_{\mathrm{hot}}$ values. However, these targets did not utilize beam smoothing and the $f_{\mathrm{hot}}$ values still remained significantly lower than predicted. It is possible that the beam quality of the current HELEN system is significantly better than that of systems operated some 20 years ago, which could account for the low data. This, however, is difficult to quantify.

Figures 1 and 2 illustrate the data for the second series of experiments. Figure 1(a) shows the measured peak radiation temperature under several conditions; Fig. 1(b) shows the corresponding measured hot electron fractions compared to those calculated from Eq. (1). The data show the radiation temperature continuing to increase as target size is reduced. Corresponding $f_{\mathrm{hot}}$ measurements show a general increase as target size is reduced, but the overall level remains relatively small. Accounting for errors in calibration, channel response, and signal unfolding, we estimate the error in the hot electron measurements to be $\pm 20\%$ absolute.

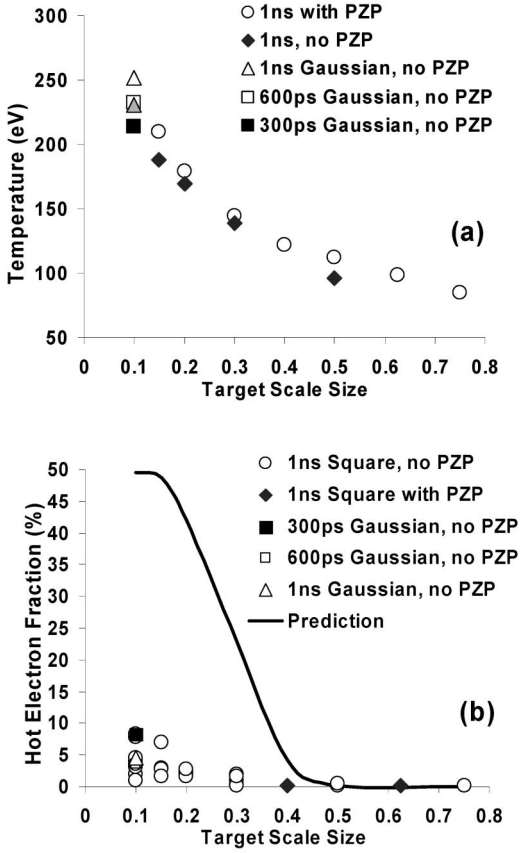


FIG. 1. Variation of hohlraum temperature (a) and hot electron fraction with target scale size (b). Also shown is the hot electron fraction predicted from Eq. (1) calculated for a 1 ns top hat pulse, variable ''C'' equal to 15 and a laser energy of 350 J.

Figures 2(a) and 2(b) show the measured SRS and SBS data, respectively, for targets shot with the 1 ns ''top hat'' laser pulse. The data show backscatter increasing to scale 0.2 and then decreasing as target size is further reduced. NBI data show no increase in backscattered light outside

TABLE I. A comparison of the theoretical and experimental data for Gaussian shaped pulses.

| Target size ($\mu$m) | Pulse length (ns) | Energy (J) | Calculated $f_{\mathrm{hot}}$ (%) | Measured $f_{\mathrm{hot}}$ (%) | Measured SRS (%) | Measured SBS (%) |
|---|---|---|---|---|---|---|
| 160 $\times$ 270 | 0.1 | 140 | 29.4 | 2.0 | 1.5 | 9.1 |
| 160 $\times$ 540 | 0.1 | 145 | 10.0 | 2.7 | 2.9 | 12.5 |
| 450 $\times$ 450 | 0.6 | 510 | 24.5 | 6.5 | 10.16 | 11.53 |
| 450 $\times$ 450 | 1.0 | 810 | 38.2 | 4.4 | 6.0 | 9.93 |
| 600 $\times$ 600 | 1.0 | 850 | 22.3 | 6.0 | 11.68 | 14.02 |

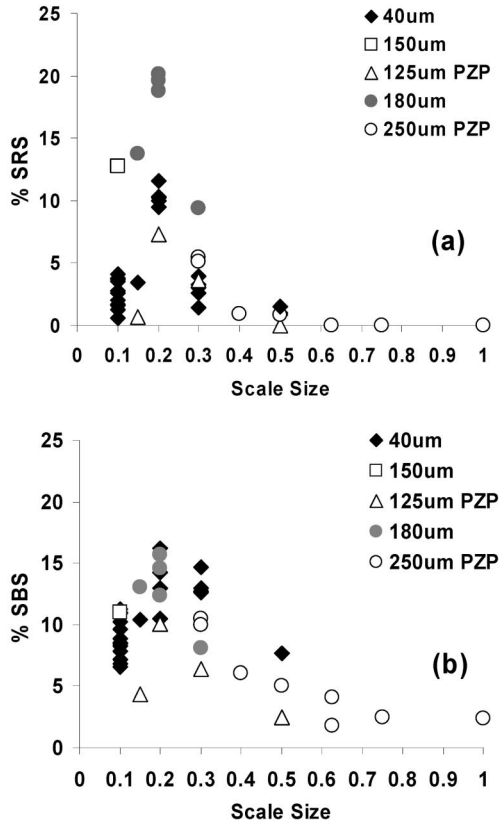


FIG. 2. Backscattered Raman (a) and Brillouin (b) data for scaled targets fired with the 1 ns ''square'' laser pulse, with and without phase plate beam smoothing.

the collection angle of the FABS as target size is reduced below scale 0.2. It is also clear that the use of phase plate beam smoothing has a significant effect on backscatter signals. This is particularly evident in the smallest targets where the size of the focal spot and hence the fraction of target wall area illuminated plays a significant role in the generation of the stimulated scatter.

Figure 3 shows the XRD measurements of the time dependent temperatures for the 1 ns top hat pulse. Peak temperature occurs at the end of the laser pulse indicating that laser energy is still being deposited within the target and not lost to parasitics.

Two-dimensional (2D) Lagrangian calculations of the radiation temperature show excellent agreement with the measured data *after* the backscattered energy was subtracted from the input energy. Figure 3 shows this agreement for scale 0.15, 0.3, and 0.75 targets. Problems with computational mesh tangling after 500 ps prevented calculations of the scale 0.1 targets from completing. In this case only the measured radiation temperature is shown.

Streaked SRS spectra for scale 0.1 targets show the signal cutting off about 400 ps after the start of the laser pulse. Calculations show that the quarter critical electron density surface (which limits the effectiveness of the SRS) reaches the LEH approximately 400 ps after the start of the laser pulse. We believe that the density and scale length of the plasma exiting the LEH drops rapidly as it expands in three dimensions, effectively stopping the SRS emission at this time. For all other scales, the quarter critical region is calculated and observed to remain within the halfraum for the duration of the laser pulse.

The SRS and SBS data in Fig. 2 show quite clearly the effects of beam smoothing on backscatter. These effects were more pronounced as the scale size decreased. The most significant effect occurs with scale 0.15 halfraums where the SRS dropped to almost zero from ~14% and the SBS signal dropped from ~13% to ~4% using a smoothed beam.

Using smoothed beams, the streaked Raman and Brillouin spectra for scale 0.15 targets showed significant changes in temporal and spectral structures. The SRS spectra show a large reduction in the measured bandwidth from approximately 300 to around 100 nm and indicate that the scattered light is tending to come from regions with electron densities around $(0.2–0.25)n_c$. The corresponding hot electron fraction data drop from ~7% to ~1.5%. There is an increase of between (6–7)% in peak temperature for all targets with the use of beam smoothing which is in good agreement with data using 0.351 $\mu$m ($3\omega$) light [26].

As it was not possible to fire the scale 0.1 hohlraum with a smoothed laser beam, the laser was defocused to fill the entire hohlraum so that a comparison could be made between illuminating a large and a comparatively small fraction of the wall area. Data in Fig. 2 show little change in the SBS signal. The SRS signal dropped from ~14% to ~4% when the beam was reduced from a diameter of ~150 to ~40 $\mu$m. The corresponding drop in the hot electron fraction was from ~4.5% to ~1.5%. This suggests that the SRS is reduced at high values of intensity times wavelength squared ($I\lambda^2$), an unexpected result. This may be due to a reduction of the filling rate with smaller first bounce spots. However, since there must be a large fraction of scattered light at such high irradiance, it is more likely this is related to the production of a hotter corona and

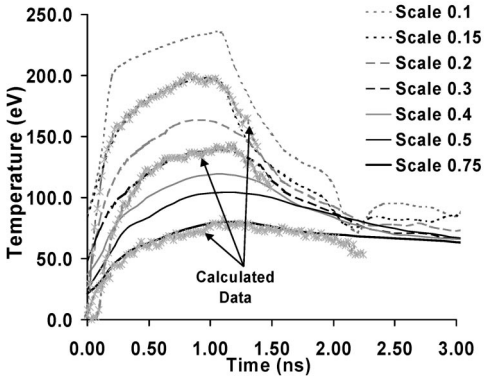


FIG. 3. Measured (using XRD) and calculated (taking backscatter into account) radiation temperature for scaled targets. The calculated data are for scale 0.15, 0.3, and 0.75 targets only.

a more rapid transit of the $0.25n_c$ density surface to the LEH than a reduction in the filling. Further evidence for this comes from the short duration of the streaked SRS signal as described earlier.

*Conclusions.*—The first series of long pulse, two sided, large hohlraums produced far lower fractions of hot electron production than had been predicted. Historical evidence for high fractions of incident energy being converted into hot electrons is based on experiments carried out at several facilities [11–16] and typically utilized a combination of either large numbers of laser beams and/or 1.06 $\mu$m light. In these experiments the incident laser light tended to be distributed over the entire surface of the hohlraum either because of the large number of beams or because the low absorption of the $1\omega$ light on first and successive bounces results in the light being repeatedly rescattered around the target. However, the targets in this experimental campaign were shot with the laser illuminating a relatively small fraction of the hohlraum wall (typically $<20\%$). It was found possible to convert a significant fraction of the incident laser energy to hot electrons (8.2%) in the most extreme case (scale 0.1 halfraum with an unsmoothed, defocused beam), but this target was expected to convert 50%. We believe that, if hot electron production is related to filling, an explanation for the data may be that the wall irradiance is sufficiently spatially peaked that the mass of blowoff is reduced and filling takes longer. Indeed, if we restrict the laser plasma generation to the laser irradiated hot spots, it is probable that the filling is dominated by more slowly expanding cold x-ray ablated plasma.

It is also possible that poor quality beams in historic experiments led to more problems with beam filamentation and the formation of regions with very high intensities which enhanced the stimulated scatter losses. We might reconcile the historic data with our results if the mechanisms for suppressing Raman and hot electron production can be overwhelmed by high $I\lambda^2$.

The HELEN experiments using very small, empty Au halfraums indicate that a change in laser intensity via beam smoothing can significantly affect both stimulated Raman and Brillouin scattering and hot electron production. Even without beam smoothing the levels of hot electron production measured were significantly lower than had been expected for the target and laser parameters used. Reducing the target scale size produced the unexpected result of a drop in both Raman and Brillouin scattering as well as the hot electron fraction.

It appears to be generally much harder than had been believed to generate hot electrons in simple axisymmetric halfraum targets using $2\omega$ light. The experimental data indicate that there is a direct correlation between the fraction of the target wall illuminated and the fraction of energy measured as hot electrons, as well as the stimulated Raman backscatter, even for these small, rapidly filling targets. The data are unequivocal in showing that the cumulative effect is to enable a traditionally ''overdriven'' target to reach temperatures much higher than would have historically been predicted through minimizing parasitic scattering processes. This is particularly evident with the smallest targets where 50% of the laser energy was predicted to be lost due to hot electrons. This would lead to a radiation temperature of $\sim$190 eV. Approximately 250 eV was measured.

The authors thank the HELEN laser operations and target fabrication staff (AWE) and Sham Dixit (LLNL).

[1] T. S. Perry *et al.*, Phys. Rev. Lett. **67**, 3784 (1991).
[2] S. D. Rothman, A. M. Evans, C. J. Horsfield, P. Graham, and B. R. Thomas, Phys. Plasmas **9**, 1721 (2002).
[3] J. M. Foster, B. H. Wilde, P. A. Rosen, T. S. Perry, M. Fell, M. J. Edwards, B. F. Lasinski, R. E. Turner, and M. L. Gittings, Phys. Plasmas **9**, 2251 (2002).
[4] R. P. Drake *et al.*, Phys. Rev. Lett. **53**, 1739 (1984).
[5] W. L. Kruer, *The Physics of Laser Plasma Interactions* (Westview Press, Cambridge, MA, 2003).
[6] T. P. Hughes, *Plasmas and Laser Light* (John Wiley and Sons, New York, 1975).
[7] J. Lindl, Phys. Plasmas **2**, 3933 (1995).
[8] J. Lindl, P. Amendt, R. Berger, S. G. Glendinning, S. Glenzer, S. Hann, R. Kauffman, O. Landen, and L. Suter, Phys. Plasmas **11**, 339 (2004).
[9] E. I. Moses, J. H. Campbell, C. J. Stolz, and C. R. Wuest, in *Optical Engineering at the Lawrence Livermore National Laboratory*, edited by P. T. Sato and M. A. Lane, Proc. SPIE Int. Soc. Opt. Eng. Vol. 5001 (SPIE–International Society for Optical Engineering, Bellingham, WA, 2003), p. 1.
[10] L. J. Suter *et al.*, Phys. Plasmas **11**, 2738 (2004).
[11] D. W Phillion, D. L. Banner, E. M. Campbell, R. E. Turner, and K. G. Estabrook, Phys. Fluids **25**, 1434 (1982).
[12] R. E. Turner, D. W Phillion, E. M. Campbell, and K. G. Estabrook, Phys. Fluids **26**, 579 (1983).
[13] R. E. Turner *et al.*, LLNL Report No. UCRL-86911, 1982.
[14] R. P. Drake *et al.*, LLNL Report No. UCRL-50021-83, 1983, pp. 5–41.
[15] D. C. Slater *et al.*, Phys. Rev. Lett. **46**, 1199 (1981).
[16] R. A. Haas *et al.*, Phys. Fluids **20**, 322 (1977).
[17] M. J. Norman *et al.*, Appl. Opt. **41**, 3497 (2002).
[18] R. M. Stevenson, M. J. Norman, T. H. Bett, D. A. Pepler, C. N. Danson, and I. N. Ross, Opt. Lett. **19**, 363 (1994).
[19] J. C. Fernandez, R. R. Berggren, K. S. Bradley, W. W. Hsing, C. C. Gomez, J. A. Cobble, and M. D. White, Rev. Sci. Instrum. **66**, 625 (1995).
[20] B. J. MacGowan *et al.*, Phys. Plasmas **3**, 2029 (1996).
[21] R. K. Kirkwood *et al.*, Rev. Sci. Instrum. **68**, 636 (1997).
[22] J. D. Kilkenny *et al.*, Rev. Sci. Instrum. **66**, 288 (1995).
[23] H. Kornblum and V. W. Slivinsky, Rev. Sci. Instrum. **49**, 1204 (1977).
[24] D. R. Kania, L. Pan, H. Kornblum, P. Bell, O. N. Landen, and P. Pianetta, Rev. Sci. Instrum. **61**, 2765 (1990).
[25] C. D. Bentley and A. C. Simmons, Rev. Sci. Instrum. **72**, 1202 (2001).
[26] S. H. Glenzer *et al.*, Phys. Plasmas **7**, 2585 (2000).